Nanotechnology **19** (2008) 075604 (5pp) doi:10.1088/0957-4484/19/7/075604

The first biopolymer-wrapped non-carbon nanotubes

Mohtashim H Shamsi and Kurt E Geckeler[1]

Laboratory of Applied Macromolecular Chemistry, Department of Materials Science and Engineering, Gwangju Institute of Science and Technology (GIST), 261-Cheomdan-gwagiro, Buk-gu, Gwangju 500-712, Korea

E-mail: keg@gist.ac.kr

Received 10 October 2007, in final form 30 November 2007
Published 31 January 2008
Online at stacks.iop.org/Nano/19/075604

Abstract

DNA-wrapped halloysite nanotubes were obtained by a mechanochemical reaction in the solid state. The characterization by scanning electron microscopy showed that the nanotubes were cut into shorter lengths and were completely covered with DNA. This resulted in a high aqueous solubility of the product with stability of the solution for about 6 weeks. The nanotubes were cut to different fractions with lengths of 200–400 nm (30–40%), 400–600 nm (10–20%) and 600–800 nm (5–10%) after ball milling. FTIR spectroscopic analysis shows that the DNA in the product remained intact. This straightforward technique for obtaining water-soluble halloysite nanotubes by a solid-state reaction has great potential for biomedical applications of nanotubes.

(Some figures in this article are in colour only in the electronic version)

1. Introduction

Halloysite ($Al_2Si_2O_5(OH)_4 \cdot 2H_2O$) is a clay mineral with a similar structure to kaolinite. Electron microscopic studies revealed that the morphology of halloysite is usually tubular. It has a 1:1 layer structure, in which the tubular morphology is achieved by layer rolling. This in turn is a dimensional misfit between the tetrahedral sheet of silica and the octahedral sheet of alumina. It covers a wide range of lengths from 0.02 to 3 μm and the diameters range from less than 50 to 200 nm [1]. Water separates the 1:1 layers from each other in halloysite. Therefore, it has a larger cation exchange capacity, surface area and catalytic activity than kaolinite [2]. It exists in both the dehydrated and hydrated form, in which layers of water molecules are situated between the successive layers. Halloysite has a wide variety of biological and non-biological applications. It has been used for storing molecular hydrogen [3], for catalytic conversions and processing of hydrocarbons [4], for removing environmental hazardous species [5], as a diuretic drug and also for urolithiasis treatment [6]. It has been characterized for microtubular drug delivery system [2] and also used for *in vitro* controlled release of different drugs [7–9]. It also shows potential to entrap both hydrophilic and hydrophobic active agents following appropriate pretreatment of the material to produce lipophilicity [10]. Not only for drug loading and release, halloysite has been shown to be an excellent hollow enzymatic nanoreactor carrying out a biomineralization process inside [11]. To date halloysite has been employed in the insoluble form in all applications. No reports on the solubilization, debundlization and dispersion in the aqueous phase have been published.

Here, we report for the first time the solubilization and dispersion of halloysite nanotubes (HNTs) by a simple technique based on the solid-state mechanochemical reaction to obtain a supramolecular adduct of HNT and DNA. This is a 'green' approach, as it is environmentally safe and no organic solvents are used. The process is an extension of the previously reported technique using carbon nanotubes that has been developed in our lab [12]. This process generates highly reactive centres by mechanical energy in the solid phase, enabling the nanotubes to interact with DNA, and results in a nanotube product with excellent dispersion properties in the aqueous phase. Nonetheless, the soluble HNT product wrapped with DNA by means of a non-covalent approach is different from the previous work, as it requires only a short time and a smaller amount of reagent (DNA) consumption. For SWNTs other DNA-wrapping approaches have also been reported [13]. In addition, halloysite has a fairly large diameter compared to that of carbon nanotubes, thus

[1] Author to whom any correspondence should be addressed.

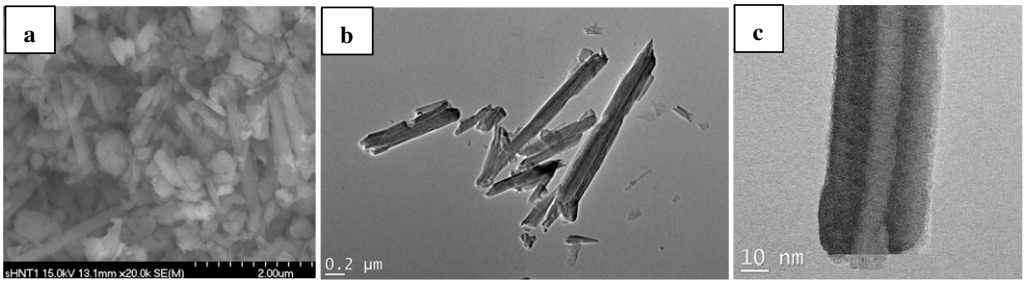

Figure 1. (a) SEM image and (b) TEM image of raw halloysite nanotubes; (c) HRTEM image showing the hollow cavity of a single HNT.

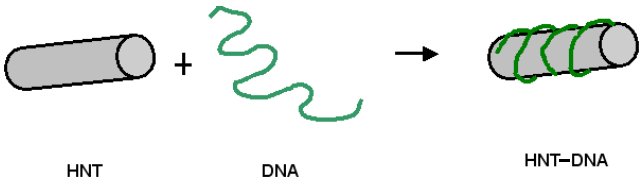

Scheme 1. Schematic of the formation of DNA-wrapped halloysite nanotubes.

opening up a different spectrum of applications. The products were characterized by FTIR, UV–vis and NIR spectroscopy, field emission scanning electron microscopy (FE-SEM) and transmission electron microscopy.

2. Experimental details

2.1. Materials

Halloysite (premium grade) was obtained from New Zealand China Clays Ltd (New Zealand). DNA (sodium salt of double-stranded DNA from herring testes) was purchased from Sigma. In all experiments doubly deionized water was used, where required. Halloysite was first sieved (125 μm mesh) to remove granules. We obtained 42% fine powder (HNT).

2.2. Synthesis of HNT–DNA conjugate

Equal amounts of the nanotubes (HNT) and DNA (50 mg) were placed in the ball milling apparatus and the mixture was milled for 1 h at room temperature (20 Hz). A very fine, homogeneous, pale-white powder was obtained, which was thoroughly shaken for 2 min in water to dissolve it. It was centrifuged (Vision centrifuge, model VS-5000N) for 30 min at 2500*g* and the supernatant product was collected. The supernatant product was then freeze-dried and used for further analysis. The residue was dried in a vacuum oven at 50 °C for 36 h. The same procedure was repeated with decreasing time intervals of 40, 30 and 20 min under the same conditions. As a control the pristine halloysite was milled for 60, 40, 30 and 20 min, respectively, in the absence of DNA (product c-HNT).

2.3. Instrumentation

Infrared spectra were recorded on a Shimadzu FTIR-8400S. Samples were prepared by making pellets with dried IR grade KBr salt. SEM images were obtained with a field emission scanning electron microscope (FE-SEM) (Hitachi Model S-4700, operating voltage; 15 kV). The powder was used as the starting material (HNT) and the freeze-dried product was used for mounting on a carbon tape. TEM images were obtained with a JEOL JEM-2100 with an accelerating voltage of 15 kV. The samples were prepared by placing a few drops on a mesh copper grid before examination. UV–vis–NIR spectra of aqueous solutions of DNA and HNT–DNA conjugate were obtained with a spectrophotometer model V-570 (JASCO, Japan).

3. Result and discussion

The pristine halloysite was purified by sieving. The SEM (figure 1(a)) and TEM (figure 1(b)) images of the pristine halloysite nanotubes (HNTs) show that the tubes of variable length, with some undefined structures, are agglomerated in parallel alignment. However, figure 1(c) is a high resolution TEM image of a single HNT, which shows the layered walls and a hollow cavity of 10 nm diameter. Also, the pristine HNTs have a very smooth surface. HNT and DNA were ball milled at room temperature. The white powder obtained was dissolved in water, centrifuged and then the supernatant solution of the conjugate product was freeze-dried. The amount of halloysite in the product was found to be 22%, which was then characterized with TEM, FTIR and UV–vis–NIR.

Scheme 1 shows the HNT wrapped with double-stranded DNA through a mechanochemical reaction. It was found that the HNT–DNA adduct synthesized for a reaction time of 60 min was stable in water for more than two months. However, the tubular structure was completely destroyed (see figure 2(b)). Similarly, the product synthesized for 40 min was also stable for almost the same period; however, the tubular structure was only partially destroyed (see figure 2(a)).

In contrast, the products synthesized for 30 and 20 min retained the tubular structure of the nanotubes, while no precipitation was observed in the diluted solution for up to six weeks. The reduced stability is attributed to the high density (2.55 g cm^{-3}) and the long tubular structure of HNTs. Figures 3(a) and (b) are the TEM images of the HNT–DNA adduct for 30 and 20 min, respectively. While the pristine HNTs show a smooth surface (see figure 1(b)), the highly dispersed HNTs wrapped with DNA around the walls of the

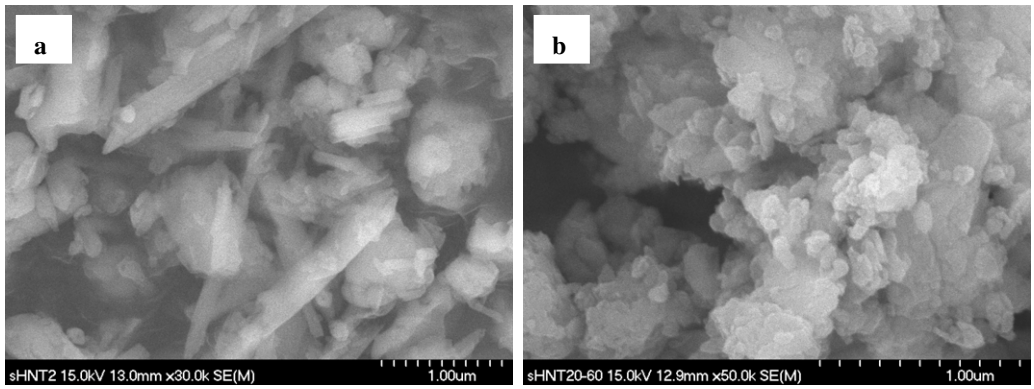

Figure 2. (a) SEM image of HNT–DNA conjugate synthesized at 40 min, 20 Hz. (b) SEM image of HNT–DNA conjugate synthesized at 60 min, 20 Hz.

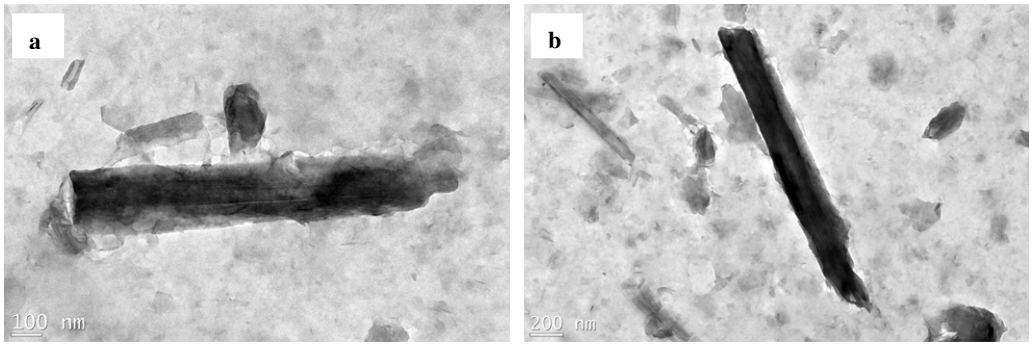

Figure 3. (a) TEM image of HNT wrapped with DNA for 30 min and 20 Hz. (b) TEM image of HNT wrapped with DNA for 20 min and 20 Hz.

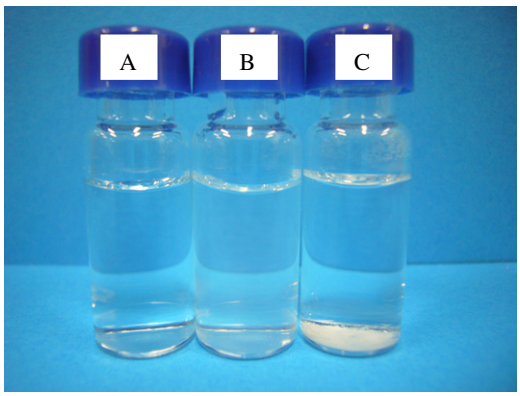

Figure 4. Photograph of the sample vials from left to right: (A) water, (B) HNT–DNA aqueous solution; 4.5 mg ml^{-1}, (C) pristine HNT; 2.1 mg ml^{-1}.

HNT look different. Figure 4 shows the water (A), water-soluble HNT–DNA conjugate (B), and insoluble HNT in water (C). The high water solubility of the product (about 10 mg ml^{-1}) is probably based on a supramolecular (π–π) interaction between the backbones of the DNA with the outer surface of the nanotubes. The phosphate side groups might also be helpful in the process of solubilization. In contrast, the pristine HNT, c-HNT, did not show any dispersion in water.

The solid-state mechanochemical reaction not only generated highly reactive centres by the mechanical energy in the solid phase, but also resulted in a shortening of the nanotubes. However, the ball milling for longer time periods can partially or totally destroy the tubular structure. Figure 5(a) shows the size distribution of the pristine halloysite nanotubes and 5(b) and (c) after ball milling for 20 min and 30 min, respectively. This illustrates the reduction in length of the long tubes between 200 and 400 nm (30–40%). The distributions between 400–600 and 600–800 nm are almost the same at around 15–25%. Evidently, there is a substantial effect of time and frequency on the milling results.

Figure 6 shows the IR spectra of HNT, DNA and the HNT–DNA product. The bands at 790 and 750 cm^{-1} in the HNT spectrum are assigned to the translational vibrations of the external OH groups as well as the out-of-plane OH bending according to the literature [14]. These bands shifted to 783 and 729 cm^{-1} in the spectrum of the product, with frequency differences of 7 and 21 cm^{-1}, respectively.

In the second spectral range between 1175 and 875 cm^{-1} (figure 7) a broad band at 1087 cm^{-1} is observed in the DNA spectrum, which is actually a combination of three unresolved overlapped bands which are distinguishable in the spectrum of the DNA [15]. These bands include 1011 cm^{-1}, which is related to the P–O or C–O backbone stretching with weak signals and also couples with the band at 1053 cm^{-1} from the same stretching. These two bands are preceded by an intense band at 1087 cm^{-1}, which is assigned to symmetric O–P–O stretching. The HNT also shows a very broad peak, like a

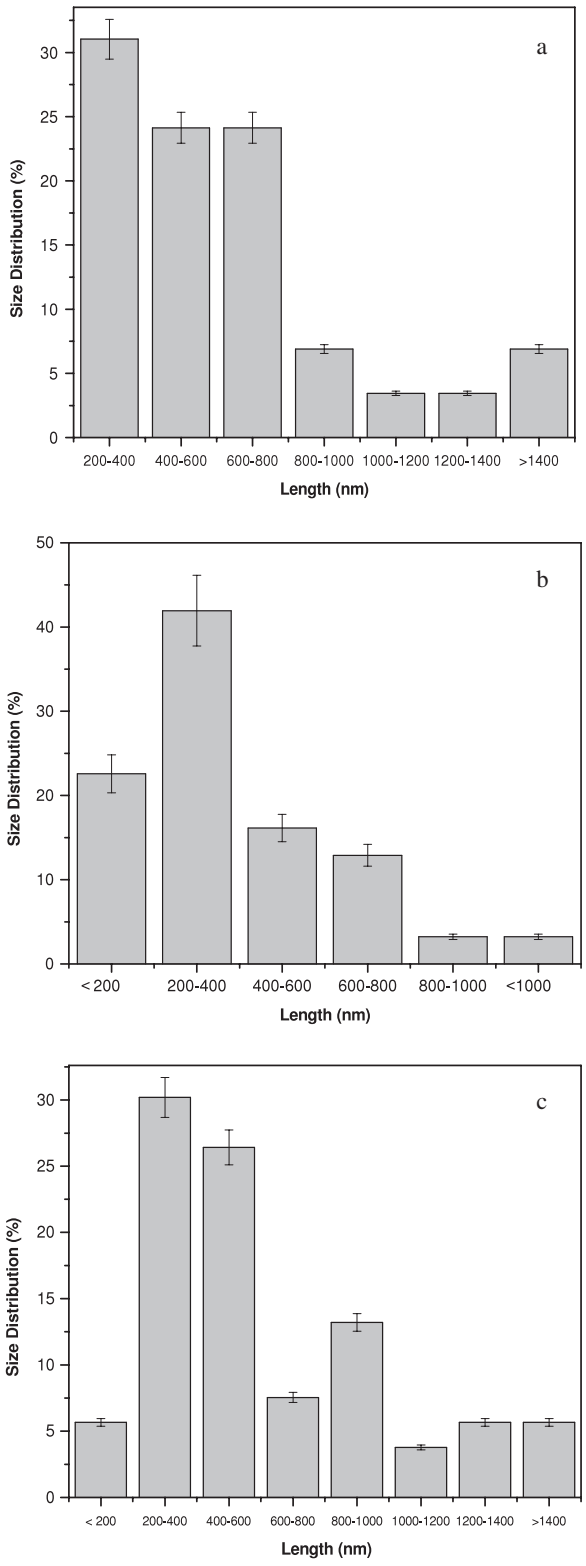

Figure 5. (a) Size distribution of the pristine halloysite nanotubes, (b) after ball milling for 20 min and (c) after 30 min.

plateau, between 1115 and 1008 cm^{-1}. This consists of three well-resolved peaks in other forms of kaolinite [16, 17]. The bands at 1033 and 1008 cm^{-1} are assigned to the Si–O–Si plane vibration and 1115 cm^{-1} to the apical Si–O vibration.

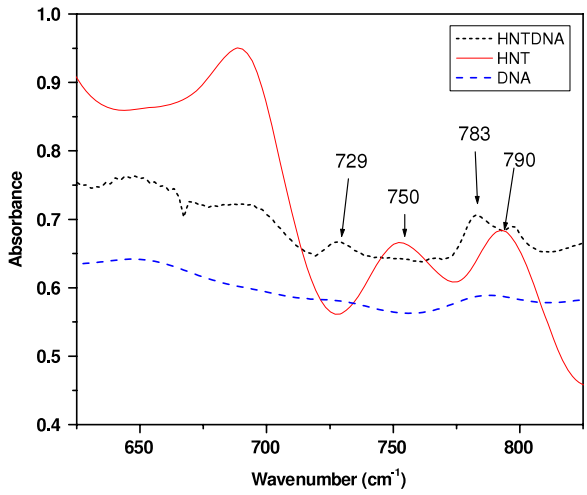

Figure 6. FTIR spectrum of HNT (solid), DNA (dashed) and HNT–DNA (dotted) in the spectral range of 850–625 cm^{-1}.

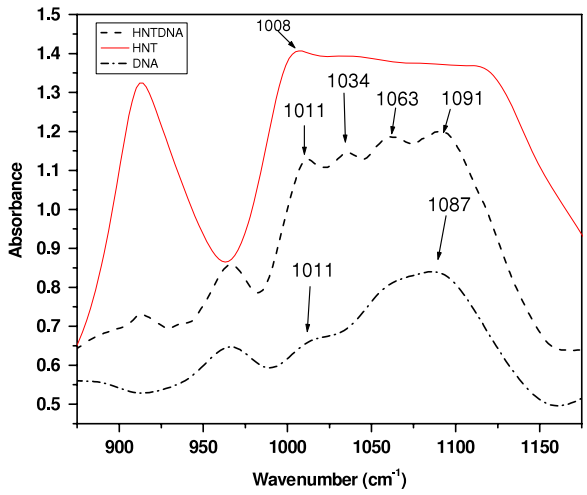

Figure 7. FTIR spectrum of HNT (solid), DNA (dash-dotted) and HNT–DNA (dashed) in the spectral range of 1175–875 cm^{-1}.

In the HNT–DNA four poorly resolved bands appeared, which are closely overlapping with each other between 1125 and 1000 cm^{-1}. The band at 1011 cm^{-1} in DNA appeared without a shift, while the 1053 and 1087 cm^{-1} bands in DNA shifted to 1063 and 1091 cm^{-1}. The peak at 1033 cm^{-1} in the HNT appeared without a significant shift. These results show structural changes in the DNA backbone due to a reorientation of the phosphate groups and an association of the phosphates in the interaction of DNA with the outer surface of the nanotubes, which is composed of silica. This significant change probably occurred due to the bending of the DNA double helix during the wrapping around the nanotubes. These findings confirm the previous studies encompassing the interaction of silica particles with DNA [15].

Figure 8 shows some other minor changes in the IR spectra. We observe two very weak bands at 1581 and 1536 cm^{-1} with a broad valley between (width: 45 cm^{-1}) in the HNT spectrum, shifted to 1560 and 1527 cm^{-1} (a difference of 21 and 9 cm^{-1}) in the product with a narrow

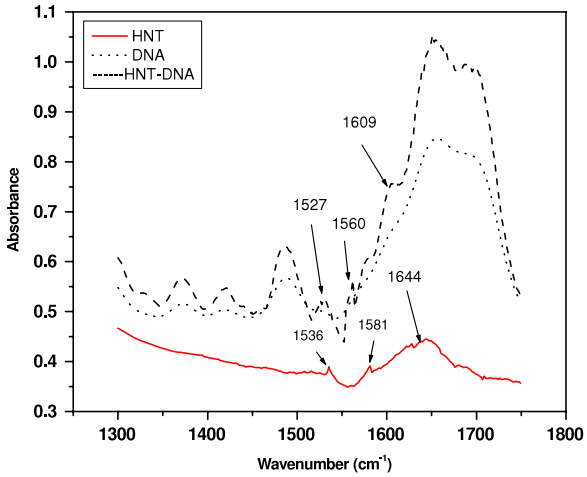

Figure 8. FTIR spectra of HNT (solid), DNA (dotted) and HNT–DNA (dashed) in the spectral range of 1750–1300 cm^{-1}.

deep valley between (width: 33 cm^{-1}). Since the middle range frequencies are correlated predominantly to the hydroxyl groups at the inner surface and the low stretching frequency is related to the inner hydroxyl groups [17] the bands are expected to correspond with the inner surface hydroxyl stretching. However, UV–vis and NIR spectroscopic results did not show significant differences.

4. Conclusion

We have described here a simple, low cost, rapid and one-pot synthetic method for the preparation of short-length, water-soluble, DNA-covered, naturally occurring aluminosilicate nanotubes by a mechanochemical reaction. This results in stabilization of the nanotubes by DNA in water for a period of about six weeks. Ball milling for 20 and 30 min cut down the length of the long tubes. The major size distribution was 200 and 400 nm (30–40%) while 400–600 nm and 600–800 nm (15–25%). However, milling for an extended period destroyed the tubular structure.

The halloysite nanotubes offer an alternative to carbon nanotubes due to their viability and low cost. Since they have diameters which are 25 to 50 times larger than those of carbon nanotubes, and also have the potential to entrap both hydrophilic and lipophilic active agents, they are excellent candidates for sustained drug delivery.

References

[1] Joussein E, Petit S, Churchman J, Theng B, Righi D and Delvaux B 2005 Halloysite clay minerals—review *Clay Miner.* **40** 383–426
[2] Levis S R and Deasy P B 2002 Characterization of halloysite for use as a microtubular drug delivery system *Int. J. Pharm.* **243** 125–34
[3] Wang X and Weiner M L 2005 Hydrogen storage apparatus comprised of halloysite *US Patent Specification* 0233199
[4] Klimkiewicz R and Edwarda B D 2004 Catalytic activity of carbonaceous deposits in zeolite from halloysite in alcohol conversions *J. Phys. Chem. Solids* **65** 459–64
[5] Lin Z and Puls R W 2000 Adsorption, desorption and oxidation of arsenic affected by clay minerals and aging process *Environ. Geol.* **39** 753–59
[6] Fushimi H, Namba T and Komatsu K 2001 Fundamental study on the quality evaluation of chinese crude drug 'Huashi' *Nat. Med.* **55** 193–200
[7] Levis S R and Deasy P B 2003 Use of coated microtubular halloysite for the sustained release of diltiazem hydrochloride and propranolol hydrochloride *Int. J. Pharm.* **253** 145–57
[8] Kelly H M, Deasy P B, Ziaka E and Claffey N 2004 Formulation and preliminary *in vivo* dog studies of a novel drug delivery system for the treatment of periodontitis *Int. J. Pharm.* **274** 167–83
[9] Byrne R S and Deasy P B 2005 Use of porous aluminosilicate pellets for drug delivery *J. Microencapsul.* **22** 423–37
[10] Price R R, Gaber B P and Lvov Y M 2001 *In vitro* release characteristics of tetracyline HCl, khellin and nicotinamide adenine dinucloetide from halloysite; a cylindrical mineral *J. Microencapsul.* **18** 713–22
[11] Shchukin D G, Sukhorukov G B, Price R R and Lvov Y M 2005 Halloysite nanotubes as biomimetic nanoreactors *Small* **1** 510–3
[12] Nepal D, Sohn J-I, Aicher W K, Lee S and Geckeler K E 2005 Supramolecular conjugates of carbon nanotubes and DNA by a solid-state reaction *Biomacromolecules* **6** 2919–22
[13] Chen R J and Zhang Y 2006 Controlled precipitation of solubilized carbon nanotubes by delamination of DNA *J. Phys. Chem.* B **110** 54–7
[14] Cuadros J and Dudek T 2006 FTIR investigation of the evolution of the octahedral sheet of kaolinite–smectite with progressive kaolinization *Clay. Clay Miner.* **54** 1–11
[15] Mao Y, Daniel L N, Whittaker N and Saffiotti U 1994 DNA binding to crystalline silica characterized by fourier-transform infrared spectroscopy *Environ. Health Perspect* **102** 165–71
[16] Deng Y, White G N and Dixon J B 2002 Effect of structural stress on the intercalation rate of kaolinite *J. Colloid Interface Sci.* **250** 379–93
[17] Ledoux R L and White J L 1964 Infrared study of selective deuteration of kaolinite and halloysite at room temperature *Science* **145** 47–9